J Appl Electrochem (2009) 39:1763–1770
DOI 10.1007/s10800-009-9875-5

ORIGINAL PAPER

The effect of catalyst support on the performance of PtRu in direct borohydride fuel cell anodes

Vincent W. S. Lam · Akram Alfantazi · Előd L. Gyenge

Received: 5 December 2008 / Accepted: 15 March 2009 / Published online: 2 April 2009

Abstract A comparative investigation of direct borohydride fuel cell polarization behavior (DBFC) was carried out with respect to the effect of unsupported and supported PtRu anode catalysts using as supports both Vulcan XC-72R and graphite felt (GF). The Vulcan XC-72R-supported catalyst alleviated mass-transfer-related problems associated with hydrogen generation from borohydride hydrolysis taking place mainly on the Ru sites. However, the most significant improvement was obtained by using the three-dimensional GF support. Typically 1.0 mg cm^{-2} PtRu was galvanostatically electrodeposited by a surfactant templated method on compressed graphite felt of 350 μm thickness. The PtRu/GF anode (Pt:Ru atomic ratio of 1.4:1) generated a DBFC peak power density of 130 mW cm^{-2} at 333 K. The separator in the DBFC was a Nafion® 117 membrane. The peak power density of the PtRu/GF was 270% and 60% higher compared with the catalyst-coated membrane configuration with unsupported PtRu and PtRu/Vulcan XC-72R, respectively.

Keywords PtRu · Borohydride · Three-dimensional electrode · Graphite felt · Direct borohydride fuel cell · Anode

1 Introduction

In recent years there has been increased interest in the development of direct borohydride fuel cells (DBFC). The necessity for liquid fuels for fuel cells arises from the complications related to hydrogen storage and distribution. Hydrogen has a low volumetric energy density at atmospheric pressure and conventional means of increasing its energy density through liquefaction or compression are either costly or too bulky for small-scale, portable electronic applications. Borohydride may be fed to the fuel cell as a liquid solution at room temperature, thus having a clear advantage over compressed hydrogen fuel for polymer electrolyte membrane fuel cells (PEMFCs) in terms of volumetric energy density (i.e., 1.86 kWh l^{-1} for 20 wt% $NaBH_4$ solution, and 0.54 kWh l_{H2}^{-1} for H_2 gas compressed at 200 atm and 298 K). Current developments in DBFC performance are comparable to those of direct methanol fuel cells (DMFC), although DBFCs are theoretically and practically superior in many ways [1, 2]. As a fuel methanol is toxic, combustible, and produces CO_2 as a byproduct; however, it is cheaper than borohydride [3]. Perhaps the most pertinent setbacks for DMFC are anode catalyst poisoning by CO_{ad} and methanol crossover to the cathode (1.12×10^{-7} mol_{CH_3OH} cm^{-2} s^{-1}) [3]. In general, organic fuels suffer from low electrooxidation catalytic activity [4].

The principal redox reactions in a direct borohydride fuel cell are as follows (standard potentials at 298 K are also given):

$$\text{Anode:}\quad NaBH_4 + 8OH^- \Leftrightarrow NaBO_2 + 6H_2O + 8e^- \qquad E_a^o = -1.24\ V_{NHE}, \tag{1}$$

$$\text{Cathode:}\quad 2O_2 + 4H_2O + 8e^- \Leftrightarrow 8OH^- \qquad E_c^o = 0.40\ V_{NHE}, \tag{2}$$

$$\text{Overall:}\quad NaBH_4 + 2O_2 \Leftrightarrow NaBO_2 + 2H_2O \qquad E_{cell}^o = 1.64\ V. \tag{3}$$

Depending upon the catalyst composition and operating conditions, the borohydride oxidation pathway may

V. W. S. Lam · A. Alfantazi · E. L. Gyenge (✉)
Department of Chemical and Biological Engineering, The University of British Columbia, 2316 Main Mall, Vancouver, BC V6T 1Z3, Canada
e-mail: egyenge@chml.ubc.ca

change. For instance, on Pt the direct oxidation of $NaBH_4$ must compete with the heterogeneous hydrolysis reaction according to reaction (4); however on Au catalysts the hydrolysis reaction is practically nonexistent [5]. Recently there have been some interest in optimizing the hydrolysis reaction for the application of indirect borohydride fuel cells (IBFC) where oxidation proceeds through reactions (4) and (5) [6–15].

$$NaBH_4 + 2H_2O \rightarrow NaBO_2 + 4H_2, \quad (4)$$

$$4H_2 + 4OH^- \rightarrow 4H_2O + 8e^- \quad E^o = -0.83\ V_{NHE}. \quad (5)$$

The hydrolysis reaction is easily activated during DBFC operation. It can be triggered by increased temperature, low NaOH concentration, and heterogeneous catalysts such as Ru, Ni, Co–B/Ni, and PtRu–$LiCoO_2$ [7, 11, 12, 14, 16, 17]. The hydrogen evolution from borohydride hydrolysis (Eq. 4) creates a countercurrent two-phase (liquid–gas) flow situation in the porous catalyst and diffusion layers as well as in the flow channels. This flow behavior leads to complications in mass transfer for typical gas-diffusion anode structures and fuel distribution methods, and it is further aggravated for larger stacks [18, 19]. In a study on the effect of hydrogen evolution on the cell and stack performances of a DBFC, Liu et al. showed that the hydrogen evolved during fuel cell operation blocks the channels in the flowfield and may also impede ion conductance at the interface between the catalyst layer and the membrane [18].

Therefore, improving the faradaic efficiency of direct borohydride oxidation to possibly $n = 8$ (Eq. 1) while minimizing the hydrogen evolution has been the focus of many investigations [5, 20, 21]. Methods that have been investigated for faradaic efficiency improvement include the addition of additives such as thiourea [5, 21], and the use of different catalysts such as AgNi, Au, and Os [5, 20, 22, 23]. Liu et al. also found that addition of Pd to the catalyst layer can suppress evolution of hydrogen [18].

To address the effect of hydrolysis (Eq. 4) on DBFC performance, in this study PtRu catalysts were investigated for borohydride electrooxidation. Ruthenium is known for its ability to heterogeneously catalyze borohydride hydrolysis [14]. An investigation conducted by Özkar and Zahmakiran on Ru nanoclusters revealed that the activation energy for borohydride hydrolysis is much lower on Ru compared with other metal catalysts: 28.5 kJ mol^{-1} for Ru versus 75 kJ mol^{-1} for Co, and 71 kJ mol^{-1} for Ni [14]. Furthermore they found that the rate of borohydride hydrolysis is linearly dependent upon the quantity of Ru nanoclusters. The addition of Ru to Pt catalyst in the DBFC would thus increase the rate of borohydride hydrolysis.

A patent by Tsang and Prasad also addresses the potential of PtRu and other anode co-catalysts for direct borohydride fuel cells [24]. According to Tsang and Prasad, the basis for PtRu is to facilitate the hydrolysis of borohydride via reaction (4) on Ru and oxidize the hydrogen on Pt via reaction (5). It is likely however that direct borohydride electrooxidation also takes place on the Pt. Duteanu et al. conducted a parametric study on a PtRu anode for DBFCs and reported power densities of up to 145 mW cm^{-2} at 333 K with a 1 mg cm^{-2} PtRu/C anode, a 1 mg cm^{-2} Pt/C cathode, and an anion exchange membrane [25]. Tsang and Prasad also emphasized the importance of controlling the operating parameters and fuel composition such that the rate of hydrogen formation does not exceed the rate of hydrogen electrooxidation [24]. A higher rate of hydrogen formation compared with electrooxidation would lead to accumulation of hydrogen gas within the anode compartment, thus creating mass-transport problems for the reactant to the catalytic sites. The accumulation of hydrogen gas in the reaction zone for DBFCs is analogous to the accumulation of carbon dioxide in the reaction zone for DMFCs. To moderate this problem, the concept of three-dimensional electrodes was also investigated [26–30]. The three-dimensional electrode consists of an electrically conductive porous substrate with thickness in a fuel cell setup between $\sim$200 and 2,000 μm, with deposited catalysts dispersed uniformly through all three dimensions of the substrate. The purpose of its original development for fuel cells by Gyenge and co-workers was to address problems associated with direct organic fuels such as CO_2 disengagement, and fuel crossover [26–29]. In addition, three-dimensional electrodes extend the reaction zone of the active layer of the fuel cell, which can improve the catalyst load utilization and hence the fuel utilization. In this study PtRu and Pt anode catalysts are compared and the effect of PtRu catalyst support (Vulcan XC-72R and graphite felt, GF) is discussed. To the authors' knowledge this is the first paper in which the application of a three-dimensional anode (e.g., PtRu/GF) for DBFCs has been introduced.

2 Experimental methods

2.1 Catalyst ink preparation

The catalyst ink used to prepare the unsupported and Vulcan XC-72R-supported PtRu catalysts consisted of a dispersion in a 2:1:4 mass ratio of: (a) catalyst powder—5 wt% Nafion® solution (3:2 catalyst powder to Nafion® dry weight ratio), (b) 15 MΩ deionized water, and (c) 2-propanol (Fisher Inc.). The ink was stirred for 5 min then sonicated for 3 h prior to use. The catalysts investigated in this study were: PtRu (1:1 at. ratio) 20 wt% supported on

Vulcan XC-72R (purchased from E-TEK), PtRu (1:1 at. ratio) black (Alfa Aesar), and Pt black (Alfa Aesar).

2.2 Fuel cell experiments

Sodium borohydride solutions were prepared using various concentrations of 98 wt% $NaBH_4$ (ACROS) and 2 M certified A.C.S. NaOH (Fisher Scientific). Supported and unsupported catalysts (1 mg cm^{-2}) were sprayed onto the membrane side of commercial cathode half membrane electrode assemblies (MEA) (Lynntech). The half MEA consisted of 4 mg cm^{-2} Pt black cathode catalyst layer painted on one side of a Nafion® 117 membrane (DuPont). Untreated carbon cloth and ELAT® gas diffusion layers were positioned between the MEA and the flowfield plates at the anode and cathode, respectively. Stainless-steel flowfield plates with serpentine flow channels compressed the MEA. Teflon-coated fiberglass gaskets (McMaster and Carr) sealed either side of the MEA. Fuel cell tests were carried out using the Fuel Cell Methanol Test Kit and FC Power™ software (Fideris).

2.3 PtRu electrodeposition on graphite felt (PtRu/GF)

A method devised by Bauer et al. for electrodeposition of PtRu nanoparticles on fibrous carbon substrates using the nonionic surfactant Triton X-100 was adopted in this study [26, 27]. The surfactant-assisted electrodeposition method generates evenly dispersed PtRu nanoparticles on graphite felts. In the present work a 350-μm-thick, 5 cm^2 geometric area compressed graphite felt (Test Solutions Inc.) was employed [27]. The felt was cleaned with methanol (Fisher) and distilled water, and then dried at 333 K in air. The electrodeposition media consisted of 65 mM $H_2PtCl_6 \cdot 6H_2O$ (99.9 wt% Aldrich), 65 mM $RuCl_3 \cdot 3H_2O$ (99.9 wt% Alfa-Aesar), and 40 wt% Triton X-100 [$C_{14}H_{22}O(C_2H_4O)_n$, $n = 9.5$] (Aldrich). Electrodeposition was carried out at a constant superficial current density (galvanostatic mode) of 6 mA cm^{-2} applied for 1.5 h using platinized titanium counterelectrodes. The temperature was 333 K. After electrodeposition the felt was rinsed with warm methanol and distilled water to remove the surfactant. The PtRu/GF was then electrochemically conditioned at −0.8 V versus Hg/Hg_2SO_4 for 5 min in 0.5 M H_2SO_4.

2.4 Characterization of the PtRu/GF

Crystallography, particle size, and phase of the deposited catalyst were identified via X-ray diffraction (XRD) using the D8 Advance Bruker diffractometer with Cu$K\alpha_1$ radiation. Transmission electron microscopy (TEM) was performed using a Hitachi H7600 microscope with an accelerating voltage of 120 kV. The TEM sample was composed of three-dimensional electrodes ground into a powder using a mortar and pestle and suspended in ethanol (Fisher Inc.).

3 Results and discussion

Figure 1a shows that the DBFC performance of PtRu black (i.e., unsupported) at 333 K is comparable to that of Pt black, reaching a peak power density of 35.1 mW cm^{-2} versus 31.6 mW cm^{-2} for Pt black. Previous electrochemical studies of the authors showed that the number of electrons for borohydride electrooxidation on PtRu/C can vary between 2 and 8 depending on the OH^-/BH_4^- concentration ratio, temperature, reaction time, electrode material, and potential [23]. A closer examination of the polarization curve in Fig. 1b reveals that borohydride electrooxidation is kinetically more favorable on PtRu than Pt. However, at current densities higher than 60 mA cm^{-2} PtRu becomes mass transport limited and the Pt performance exceeds that of PtRu. This is due to the mass-transport limitations generated by the accumulation of hydrogen gas in the PtRu anode compartment [23].

3.1 Effect of the Vulcan XC-72R support

In Fig. 2 the polarization curves for PtRu black and Vulcan XC-72R-supported PtRu are compared, both with a 1 mg cm^{-2} load. It is evident that the electrode kinetic performances are virtually identical at low current densities (up to 20 mA cm^{-2}). At higher superficial current densities there is a significant drop in performance for the unsupported catalyst. Kim et al. investigated the effect of carbon support for Pt catalysts, and found that an anode catalyst load four times higher was required for unsupported Pt catalyst to match the fuel cell performance for supported Pt catalyst [31]. Their justification for the performance difference was increased catalytic activity due to the effect of the carbon support.

It is unlikely that in our case the intrinsic electrocatalytic activity of PtRu or catalyst-support electronic interaction effects were the primary contributors to the observed differences in performance in polarization curves at current densities higher than 20 mA cm^{-2} (Fig. 2). The superior performance of the PtRu/C catalyst could be attributed to effects associated with H_2 generation by the hydrolysis reaction (Eq. 4). The supported catalyst layer is thicker in comparison with the unsupported catalyst layer due to both the carbon presence and the larger amount of Nafion®. Since the Nafion® content of the catalyst layer was measured against the total catalyst powder weight (Sect. 2.1), the weight ratio of Nafion® to metal content differed for the unsupported and supported catalyst layers; it was 3:2

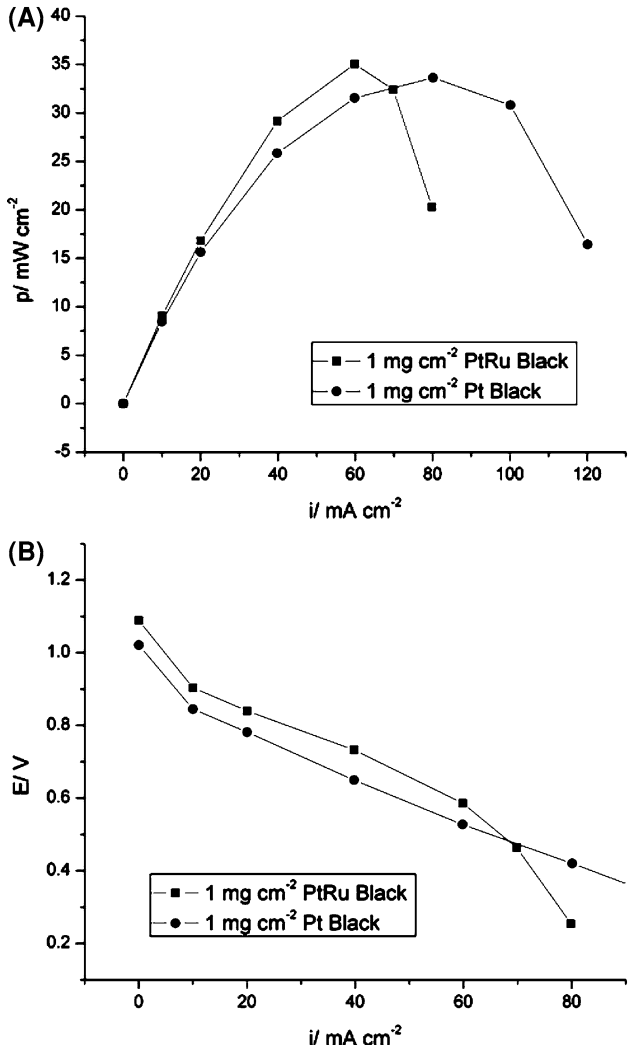

Fig. 1 Pt and PtRu anode catalyst comparison for DBFC. **a** Power density curves. **b** Polarization curves. Fuel: 0.5 M $NaBH_4$–2 M NaOH; fuel flowrate: 10 mL min^{-1}; O_2 flowrate: 1.25 L min^{-1}; P_{O_2}: 50 psig; *T*: 333 K

Nafion® to PtRu metal for the unsupported catalyst, and 15:2 for the supported catalyst.

We propose that the morphology of the thicker supported catalyst layer is such that the evolved hydrogen from the catalytic sites (mostly Ru) can be trapped more easily, and the path for the evolved hydrogen to escape would be tortuous. Thus, hydrogen will have a longer residence time inside the catalyst layer and a better chance to reach the oxidative catalytic sites (Pt). Hence, the electrooxidation of hydrogen is more efficient in the supported catalyst layer. More specifically, the relative rate of hydrogen oxidation (on Pt) with respect to hydrogen generation (by borohydride hydrolysis on Ru) is higher in the case of the supported catalyst due to both different porous electrode structure and higher Nafion® content. It must be noted that Nafion® lowers the heterogeneous hydrogen evolution rate caused by borohydride hydrolysis.

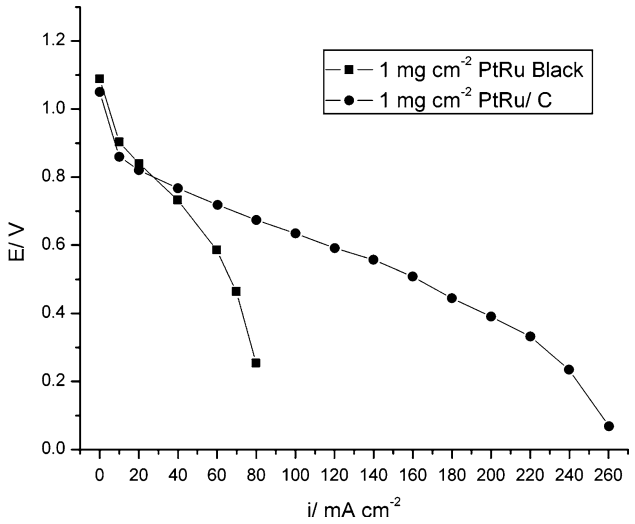

Fig. 2 Comparison of supported and unsupported catalyst performance. Fuel: 0.5 M $NaBH_4$–2 M NaOH; fuel flowrate: 10 mL min^{-1}; O_2 flowrate: 1.25 L min^{-1}; P_{O_2}: 50 psig; *T*: 333 K

Visual observations (Fig. 3a, b) of the hydrogen evolution without polarization revealed the formation at a high rate of large gas bubbles on PtRu black compared with PtRu/Vulcan XC-72R. Thus, the amount of Nafion® and carbon support can have a major effect on the rate of borohydride hydrolysis. In future studies, a quantitative comparative measurement of the hydrogen evolution rate is required under both open-circuit and anodic polarization conditions.

Kim et al. investigated the effect of Nafion® content on the anode and found an optimal composition at 30 wt%, which is in agreement with conclusions regarding hydrogen polymer electrolyte fuel cells [31, 32]. The effect of Nafion® in the case of the alkaline borohydride fuel cell was explained by the ability of Nafion® to improve the wetting of the catalyst layer, while at higher than optimum Nafion® load the ionic and electronic conductivities of the catalyst layer are diminished and hence the fuel cell performance is worse. In addition, encapsulation of catalyst particles with Nafion® may hinder mass transport of borohydride anions to catalytic sites. Cheng et al. confirmed that catalyst utilization was heavily dependent upon Nafion® content and morphology [33].

3.2 Effect of the anode structure: three-dimensional graphite felt support

Hydrogen formation can hinder mass transport of borohydride to the catalytic sites and diminish the effective ionic conductivity in the active layer [18]; therefore, it must be efficiently oxidized on Pt. One research group addressed this problem by using nickel mesh as a backing layer to facilitate the unconsumed hydrogen gas disengagement

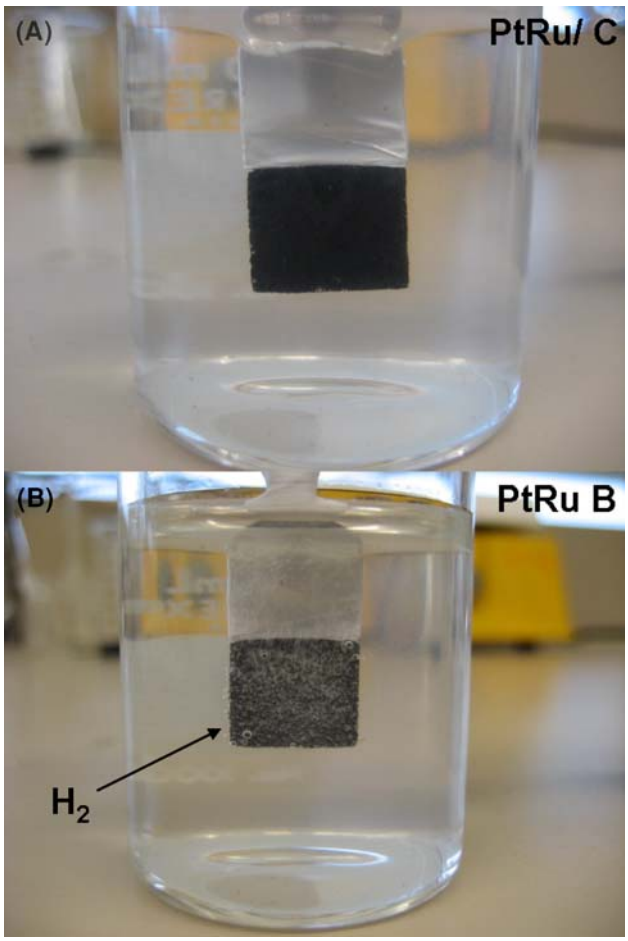

Fig. 3 Heterogeneous catalysis of borohydride hydrolyis without electrode polarization. **a** PtRu/C and **b** PtRu black. Catalyst sprayed on Toray carbon paper with Nafion® binder. Solution: 0.5 M $NaBH_4$–2 M NaOH; *T*: 293 K

formed on titanium-mesh supported anodes [30]. A major advantage of using a three-dimensional anode in DBFC besides providing an extended reaction zone for borohydride oxidation is the high macroporosity of the felt (e.g., ≥90%), which can aid in the disengagement of unconsumed hydrogen with lesser interference on the liquid mass transfer. Furthermore, ionic conductance from the reaction sites to the membrane is provided by the concentrated NaOH electrolyte typically present also for stabilizing the borohydride. Thus, another advantage is the absence of Nafion® in the three-dimensional anode structure, which would mitigate such complications as electrical insulation of the catalyst particles, and potential mass-transport limitations of BH_4^- anions diffusing through the Nafion® film. The graphite felt electrode may also help reduce the high borohydride crossover rate (e.g., 4.01×10^{-7} mol cm^{-2} s^{-1} using the Nafion® 117 membrane [3]) due to its extended reaction zone thickness of 350 μm coupled with possibly higher catalyst utilization and activity.

3.2.1 *Characterization of PtRu supported on 3-D graphite felt*

Figure 4a and b show TEM pictures of catalyst particles on the graphite felt three-dimensional electrode produced by surfactant templated electrodeposition (Sect. 2.3). The larger deposits (e.g., ∼160 nm in diameter) (Fig. 4a) are in fact agglomerates of much smaller particles with a narrow size distribution ranging from 2.9 to 4.6 nm, creating a microporous catalyst structure (Fig. 4b).

Figure 5 shows the XRD pattern of the PtRu alloy. The particle sizes were calculated using:

$$d = \frac{\kappa\lambda}{\beta \cos\theta}, \tag{6}$$

where d is the particle diameter in Å, κ is a coefficient equal to 0.88, λ is the X-ray wavelength equal to 1.54058 Å, β is the full-width at half-maximum (FWHM) in radians, and θ is the angle at the maximum peak in radians.

The particle sizes were found to range from 3.7 to 4.5 nm. Broadening of the XRD peaks, shift of the Bragg angle, and decrease of the lattice parameter may suggest the presence of PtRu alloy.

From inductively coupled plasma atomic emission spectroscopy (ICP-AES) the Pt atomic composition was $x = 0.583$ [34], corresponding to a lattice parameter of 3.885 Å for the PtRu alloy:

$$a_{\mathrm{PtRu}} = x a_{\mathrm{Pt}} + (1 - x) a_{\mathrm{Ru}}, \tag{7}$$

where a is the lattice parameter and x is the atomic fraction of Pt.

The calculated lattice parameter is corroborated by the results of Lalande et al. [35]. Interpolating their bulk data for a $Pt_{0.583}Ru_{0.417}$ alloy the PtRu lattice parameter is 3.881 Å.

Thus, there is good indication for the presence of PtRu alloy, but it cannot be considered conclusive evidence. The XRD results for PtRu alloy could also be confused with a mixture of face-centered cubic (fcc) Pt and Ru catalysts, or a mix between PtRu alloy and fcc Pt and Ru catalysts. In order to prove the presence of PtRu alloy several PtRu compositions have to be tested with a Ru content no greater than 0.62, due to the formation of the hexagonal close-packed (hcp) phase in which Ru atoms are replaced by Pt atoms [36]. The results must then obey the linearity of Vegard's law.

Calculation of the specific surface area based on the particle size yielded an average of 82.34 m^2 g^{-1}.

3.2.2 *Three-dimensional graphite felt anode performance in DBFC*

Figure 6a compares the performance of unsupported PtRu (i.e., PtRu black), Vulcan XC-72R-supported PtRu (i.e.,

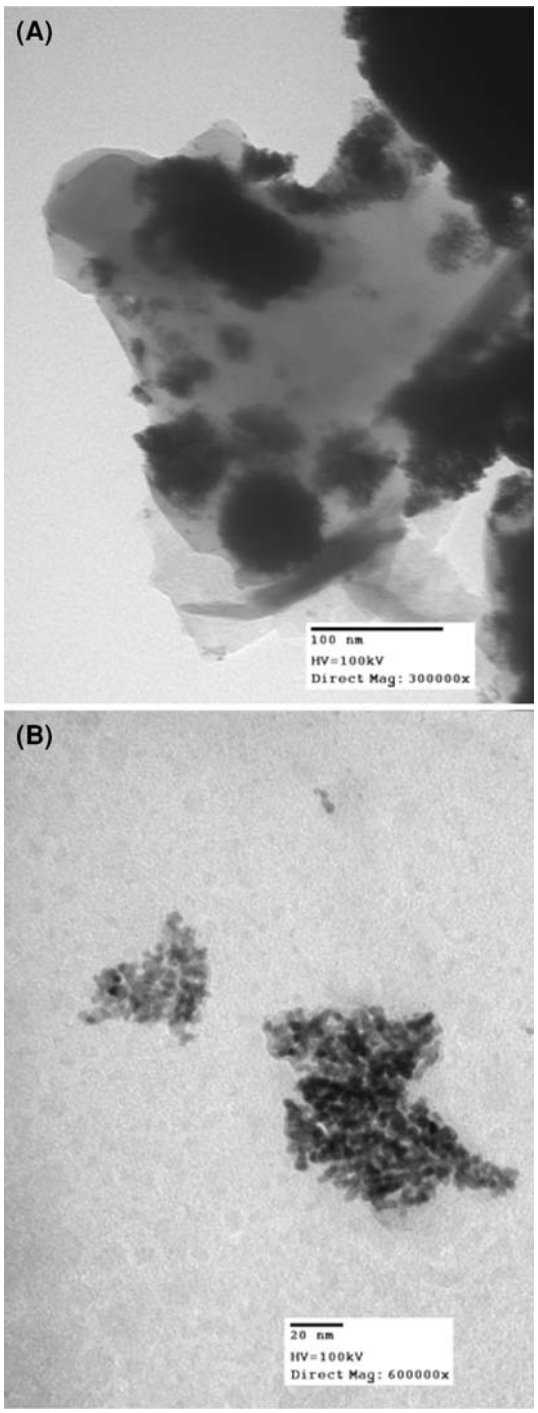

Fig. 4 TEM pictures of PtRu electrodeposited on compressed graphite felt: **a** 3×10^5 magnification, **b** 6×10^5 magnification

PtRu/C), and the PtRu/GF. Generating a peak power density of 130 mW cm^{-2} the three-dimensional electrode enhanced the performance of the DBFC by approximately 33% compared with the conventional catalyst-coated membrane (CCM), having a fourfold higher unsupported

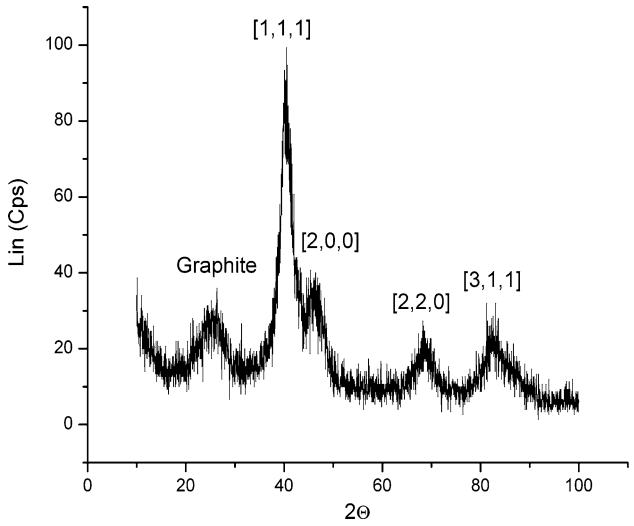

Fig. 5 XRD spectra of PtRu electrodeposited on compressed graphite felt

PtRu load. Compared with unsupported and Vulcan XC-72R-supported PtRu at the same loading (1 mg cm^{-2}), the performance improvement with PtRu/GF based on peak power density was approximately 270% and 60%, respectively.

The open-circuit voltage was the lowest (i.e., 0.99 V) for the PtRu black with the highest load (4 mg cm^{-2}), followed by PtRu/C at 1.05 V, and finally PtRu/GF at 1.11 V. This can be explained by the higher Ru content of the 4 mg cm^{-2} CCM. It is likely that such a high loading of Ru, approximately 1.3 mg cm^{-2}, promotes the hydrolysis reaction (4) to such an extent that the open-circuit voltage becomes more dependent on the hydrogen reversible potential.

From Fig. 6b it is clear that borohydride electrooxidation on the three-dimensional electrode was favorable compared with CCMs for all the investigated cases and over the entire polarization curve. The open structure of the three-dimensional electrode is better suited for the countercurrent two-phase gas–liquid flow regime and permits the unconsumed hydrogen gas to escape more easily without blocking the liquid feed pathways to the reaction sites. Furthermore, efficient gas evolution has the positive effect of enhancing the liquid mass-transfer rate close to the electrode surface. All these factors contribute to the fact that, as Fig. 6 indicates, for PtRu/GF clear mass-transfer limitation is not apparent in the polarization curves at least up to 450 mA cm^{-2}, whereas for PtRu/C and PtRu black with the same catalyst load of 1 mg cm^{-2} the mass-transfer-limiting superficial current densities are approximately 260 mA cm^{-2} and 75 mA cm^{-2}, respectively.

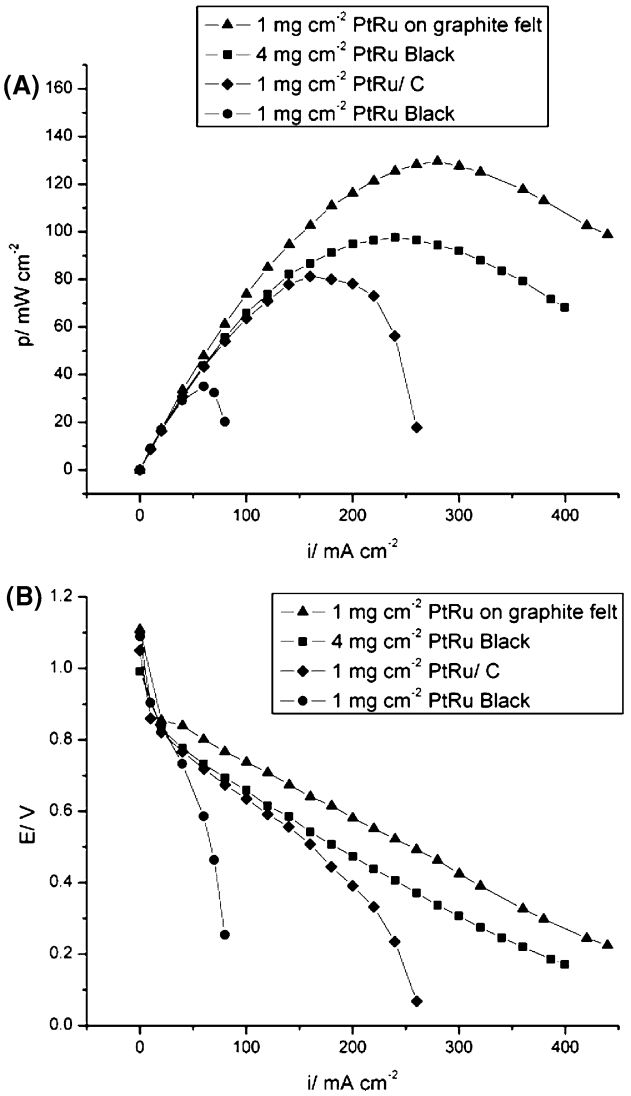

Fig. 6 Effect of the three-dimensional anode structure on the DBFC. **a** Power density curves. **b** Polarization curves. Fuel: 0.5 M $NaBH_4$–2 M NaOH; fuel flowrate: 10 mL min^{-1}; O_2 flowrate: 1.25 L min^{-1}; P_{O_2}: 50 psig; *T*: 333 K

4 Conclusion

The improved performance of PtRu/C (Vulcan XC-72R) versus PtRu black anode catalysts in DBFC was attributed to mass-transport effects and different catalyst layer morphology due to the support. The thicker PtRu/C catalyst layer is characterized by more tortuous pathways for hydrogen evolution. Therefore, the hydrogen generated mainly by borohydride hydrolysis on the Ru sites is retained for longer durations in the catalyst layer where hydrogen electrooxidation takes place on the Pt sites. In contrast, the thin PtRu black catalyst layer is quickly saturated with evolved hydrogen gas, shielding the electrode surface and blocking the borohydride access. The borohydride electrooxidation reaction mechanism on PtRu is dominated by indirect oxidation of borohydride (i.e., via hydrogen). Hence, PtRu is a bifunctional catalyst for borohydride oxidation.

Hydrogen retention in the catalyst layer can cause a number of problems in the DBFC, such as hampering the borohydride mass transfer leading to low fuel utilization efficiency, low effective ionic conductivity across the catalyst layer that increases the ohmic voltage loss, and high anode pressure that could aggravate the borohydride crossover rate across the membrane. In future studies the hydrogen evolution rate must be experimentally measured under both nonpolarized and anodic polarization conditions.

The application of a monolithic three-dimensional graphite felt anode with electrodeposited PtRu (i.e., PtRu/GF) significantly increased the peak power density of the DBFC. At 333 K the PtRu/GF with 1 mg cm^{-2} PtRu generated peak power of 130 mW cm^{-2} at 275 mA cm^{-2}, while under similar conditions with PtRu/C (Vulcan XC-72R) the peak power was only 80 mW cm^{-2}, corresponding to a superficial current density of 150 mA cm^{-2}. It must be noted that a cation exchange membrane (Nafion® 117) was employed in the present work. The use of an anion exchange membrane would improve the ionic conductivity and therefore the fuel cell performance [25]. However, anion exchange membranes are typically less robust and more costly.

The performance enhancement with the graphite felt three-dimensional support was attributed mainly to the enhanced two-phase (liquid borohydride/hydrogen gas) mass transfer in the anode compartment. Thus, the three-dimensional anode design in the context of the borohydride fuel cell constitutes a promising engineering advancement for the improvement of the power density while lowering the anode catalyst load.

Acknowledgements The authors would like to acknowledge the financial support of this work by the Natural Science and Engineering Research Council of Canada and the Auto 21 NCE Program. The authors would also like to acknowledge Alex Bauer for his aid in the surfactant templated electrodeposition of PtRu on graphite felt.

References

1. Amendola SC, Onnerud P, Kelly MT, Petillo PJ, Sharp-Goldman SL, Binder M (1999) J Power Sources 130:133
2. Li ZP, Liu BH, Arai K, Suda S (2005) J Alloys Compd 648:652
3. Wee J (2006) J Power Sources 1:10
4. Cheng H, Scott K (2006) J Power Sources 407:412
5. Gyenge E (2004) Electrochim Acta 965:978
6. Xu D, Dai P, Liu X, Cao C, Guo Q (2008) J Power Sources 616:620
7. Dai H, Liang Y, Wang P, Cheng H (2008) J Power Sources 17:23
8. Amendola SC, Sharp-Goldman SL, Janjua MS, Kelly MT, Petillo PJ, Binder M (2000) J Power Sources 186:189

9. Amendola SC, Sharp-Goldman SL, Janjua MS, Spencer NC, Kelly MT, Petillo PJ, Binder M (2000) Int J Hydrogen Energy 969:975
10. Park J, Shakkthivel P, Kim H, Han M, Jang J, Kim Y, Kim H, Shul Y (2008) Int J Hydrogen Energy 1845:1852
11. Krishnan P, Yang T, Lee W, Kim C (2005) J Power Sources 17:23
12. Krishnan P, Hsueh K, Yim S (2007) Appl Catal B 206:214
13. Walter JC, Zurawski A, Montgomery D, Thornburg M, Revankar S (2008) J Power Sources 335:339
14. Özkar S, Zahmakıran M (2005) J Alloys Compd 728:731
15. Keçeli E, Özkar S (2008) J Mol Catal A Chem 87:91
16. Liu BH, Li ZP, Suda S (2004) Electrochim Acta 3097:3105
17. Indig ME, Snyder RN (1962) J Electrochem Soc 1104:1106
18. Liu BH, Li ZP, Zhu JK, Suda S (2008) J Power Sources 151:156
19. Kim C, Kim K, Ha MY (2008) J Power Sources 154:161
20. Feng RX, Dong H, Cao YL, Ai XP, Yang HX (2007) Int J Hydrogen Energy 4544:4549
21. Martins JI, Nunes MC, Koch R, Martins L, Bazzaoui M (2007) Electrochim Acta 6443:6449
22. Dong H, Feng R, Ai X, Cao Y, Yang H, Cha C (2005) J Phys Chem B 10896:10901
23. Lam VWS, Gyenge EL (2008) J Electrochem Soc B1155:B1160
24. Tsang JW, Prasad R (2003) Co-catalyst proton exchange membrane fuel cell utilizing borohydride fuels. Patent No. US6982128 B2
25. Duteanu N, Vlachogiannopoulos G, Shivhare M, Yu E, Scott K (2007) J Appl Electrochem 1085:1091
26. Bauer A, Gyenge EL, Oloman CW (2007) J Power Sources 281:287
27. Bauer A, Gyenge EL, Oloman CW (2006) Electrochim Acta 5356:5364
28. Cheng TT, Gyenge EL (2006) Electrochim Acta 3904:3913
29. Lycke DR, Gyenge EL (2007) Electrochim Acta 4287:4298
30. Cheng H, Scott K (2006) J Appl Electrochem 1361:1366
31. Kim J, Kim H, Kang Y, Song M, Rajendran S, Han S, Jung D, Lee J (2004) J Electrochem Soc A1039:A1043
32. Paganin VA, Ticianelli EA, Gonzalez ER (1996) J Appl Electrochem 297:304
33. Cheng X, Yi B, Han M, Zhang J, Qiao Y, Yu J (1999) J Power Sources 75:81
34. Bauer AG (2008) Dissertation: direct methanol fuel cell with extended reaction zone anode: PtRu and PtRuMo supported on fibrous carbon. The University of British Columbia, Canada
35. Lalande G, Denis MC, Guay D, Dodelet JP, Schulz R (1999) J Alloys Compd 301:310
36. Antolini E, Giorgi L, Cardellini F, Passalacqua E (2001) J Solid State Electrochem 131:140